COBEM 2023 27TH INTERNATIONAL CONGRESS OF MECHANICAL ENGENEERING

ABCM Brazilian Society of Mechanical Sciences and Engineering
27th ABCM International Congress of Mechanical Engineering
December 04-08, 2023, Florianópolis-SC, Brazil

COB-2023-2027
NUMERICAL STUDY OF SLOT COATING FLOWS WITH A VISCOUS LIQUID-GAS INTERFACE

Filipe Oliveira da Silva
Department of Mechanical Engineering, Universidade Federal do Rio de Janeiro, Rio de Janeiro, RJ 21941-972, Brazil
filipeoliveira@mecanica.coppe.ufrj.br

Ivan Rosa de Siqueira
Department of Chemical and Biomolecular Engineering, Rice University, Houston, Texas 77005, USA
irs@rice.edu

Márcio da Silveira Carvalho
Department of Mechanical Engineering, Pontificia Universidade Catolica do Rio de Janeiro, Rio de Janeiro, RJ 22451-900, Brazil
msc@puc-rio.br

Roney Leon Thompson
Department of Mechanical Engineering, Universidade Federal do Rio de Janeiro, Rio de Janeiro, RJ 21941-972, Brazil
rthompson@mecanica.coppe.ufrj.br

Abstract. *Slot coating is a widely used and highly precise manufacturing method that applies a thin liquid film onto a solid surface, also known as the substrate, at a constant velocity. We employ the equations of motion for incompressible Newtonian liquids in bulk flow coupled with the Boussinesq-Scriven constitutive equation for viscous interfaces in the dynamic boundary condition at the liquid-air free surface. The problem is then solved using Finite Element Method with elliptic mesh generation and Galerkin's weighted residuals. We conduct a parametric study of slot coating flows with a viscous liquid-gas interface in order to determine the viscous interface influence for different Capillary and Boussinesq numbers at different flow rates. The results reveal that when the interfacial viscosity increases, the meniscus curvature reduces regardless of capillary number, i.e., surface tension. As the free surface bends less, it also requires more substrate length for the film to achieve rigid-body movement, thus influencing the streamwise velocity and the liquid acceleration along the free surface.*

Keywords: *Slot coating, low-flow limit, Boussinesq-Scriven model, finite element method, viscous interface.*

1. INTRODUCTION

Multiphase interfaces, particularly fluid-fluid interfaces, appear in all kinds of processes, from natural and biological ones to those used in industry. We can find complex fluid-fluid interactions for example in food, environment, living systems, and industrial processes. Free surface flows at fluid-fluid interfaces are particularly important in manufacturing processes like extrusion flow and liquid coating.

Slot coating is a well-known high-precision manufacturing method that is commonly used on a broad variety of products such as adhesive, magnetic tapes, and flexible displays. Recent studies have also showcased the capability of slot coating in producing high-performance coatings for energy devices, ranging from lithium-ion batteries (Schmitt *et al.*, 2013, 2014, 2015) to perovskite solar cells (Rong *et al.*, 2018; Whitaker *et al.*, 2018; Verma *et al.*, 2020). It entails continually depositing a thin liquid film over a solid surface known as the substrate while moving at a constant velocity. A slight vacuum is applied to the gas from the upstream meniscus as a means to stabilize the coating bead at higher velocities (Beguin, 1954). This technique falls under the category of coatings known as pre-metered coatings, in which the thickness of the coated layer can be determined based on the substrate speed and the flow rate of the liquid fed into the coating die, both of which are independent of the rheological properties of the coating liquid (Sartor, 1990).

Modeling coating flows is a challenging task. This assertion is supported by factors such as menisci and moving boundaries at gas-liquid interfaces, static and dynamic contact lines where different phases meet, and the fact that coating is widely used with non-Newtonian fluids with complex rheology. Despite the fact that computational solutions have proven to be effective and trustworthy, the effects of interfacial rheology of processing flows have yet to be thoroughly investigated in the literature. In this regard, the rheological behavior of fluid-fluid interfaces should play a significant role in these applications, which this work intends to study. A review of computational rheology and fundamentals and applications of interfacial rheology are presented in Jaensson *et al.* (2021), Fuller and Vermant (2012) and Jaensson and

Vermant (2018).

Previous theoretical, experimental, and computational studies extensively examined the fundamental aspects of slot coating flows, focusing on Newtonian liquids (Lee and Liu, 1992; Carvalho and Kheshgi, 2000; Chang *et al.*, 2007; Lee and Nam, 2015; Benkreira and Ikin, 2016; Yoon *et al.*, 2022; Kwak and Nam, 2022; Silva *et al.*, 2023) and several non-Newtonian systems (Pasquali and Scriven, 2002; Romero *et al.*, 2004, 2006; Bajaj *et al.*, 2008; Lee *et al.*, 2011; Lee and Nam, 2017; Khandavalli and Rothstein, 2016; Campana *et al.*, 2017; Siqueira *et al.*, 2017; Rebouças *et al.*, 2018; Siqueira and Carvalho, 2019; Kwak and Nam, 2020). These investigations firmly established the significance of the coating liquid's rheology in slot coating flows. However, existing analyses have been mostly limited to flows with rheologically simple interfaces. In practice, many coating liquids contain surface-active components like nanoparticles and surfactants, leading to rheologically complex interfaces. These complex interfaces exhibit viscous, elastic, and/or plastic responses under deformation, which impact the stress balance and the stability of free surfaces. Therefore, understanding the rheology of fluid interfaces is crucial for slot coating applications. For example, recent studies have already shown that viscous interfaces have a substantial effect on planar extrudate swell flows (Mendes Junior *et al.*, 2021) and on slot coating flows and its coating window (Silva *et al.*, 2023).

In this study, we conduct a computational investigation into the behavior of free surface flows, focusing on the formation of a liquid film within the downstream segment of a slot coater. Our model incorporates the equations governing the motion of incompressible Newtonian liquids within the bulk flow, coupled with the Boussinesq–Scriven constitutive equation (Boussinesq, 1913; Scriven, 1960), designed for purely viscous interfaces resembling Newtonian behavior. This model stands as one of the earliest constitutive relationships for complex interfaces, presenting a surface analogy to the conventional Newtonian model applied to bulk fluids and has been extensively applied in studying a wide range of interfacial flow phenomena, such as dynamics involving droplets (Narsimhan, 2018, 2019; Singh and Narsimhan, 2020), threads (Martínez-Calvo and Sevilla, 2018, 2020; Wee *et al.*, 2020), and fingering instabilities in porous media (Li and Manikantan, 2021; Conrado *et al.*, 2023; Coutinho *et al.*, 2023). A mixed finite element approach is then used to solve the equations of motion and boundary conditions for free surface flows after they are further connected with the elliptic mesh generation method.

2. PROBLEM FORMULATION

2.1 Governing equations

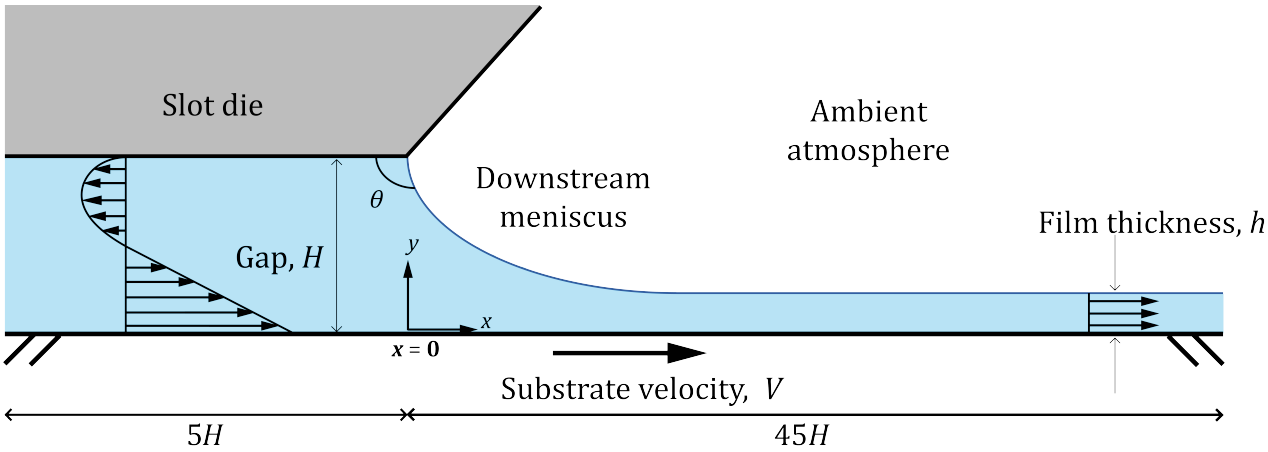

Figure 1. 1. Sketch of the problem (not to scale)

It is a reasonable assumption to model slot coating as a planar two-dimensional problem. Since the important flow events which we are interested in only take place after the coating bead, we will only use the downstream section of the flow. We assume the flow is isothermal and incompressible and that the inertial and gravitational effects are negligible due to the small length scales in slot coating flows. Thus, the equations of mass conservation and momentum balance for an incompressible Newtonian fluid are:

$$\nabla \cdot \mathbf{u} = 0 \tag{1}$$

$$\nabla \cdot \mathbf{T} = 0 \tag{2}$$

$$\mathbf{T} = -p\mathbf{I} + \mu(\nabla\mathbf{u} + \nabla\mathbf{u}^T) \tag{3}$$

where, in the equations above, $\mathbf{u}$ is the velocity field, $\mathbf{T}$ is the liquid stress tensor, p is the modified mechanical pressure, $\mathbf{I}$ is the identity tensor and μ is the bulk fluid viscosity.

The boundary conditions used to solve the continuity and momentum equations are:

1. No-slip and no-penetration boundary conditions at solid walls. Thus, $\mathbf{u} = 0$ at die walls and $\mathbf{u} = \mathrm{V}\,\hat{\mathbf{e}}_\mathbf{1}$ at the substrate, where $\hat{\mathbf{e}}_\mathbf{1}$ is the unit vector at the x direction.
2. Imposed velocity profile at the inlet, where $\mathbf{u}$ is a contribution of a Couette and a Poiseuilli flow: $\mathbf{u} = [[6(\frac{q}{H} - \frac{V}{2})\frac{y}{H} + V](1 - \frac{y}{H})]\hat{\mathbf{e}}_\mathbf{1}$
3. No-flow boundary condition at the outlet, as detailed in Papanastasiou *et al.* (1992).
4. At the free surface interface, the interfacial force balance is given by $\hat{\mathbf{n}} \cdot \sigma_\mathbf{s} = -p_0\hat{\mathbf{n}} + \nabla_s \cdot \sigma_\mathbf{s}$, as per Mendes Junior *et al.* (2021) and Silva *et al.* (2023). Where, in the boundary condition equation, $\hat{\mathbf{n}}$ is the local unit normal vector, $\sigma_\mathbf{s}$ is the interfacial stress tension, p_0 is the outer gas pressure, the gradient interfacial operator $\nabla_s = \mathbf{I_s} \cdot \nabla$ and the projection tensor $\mathbf{I_s} = \mathbf{I} - \hat{\mathbf{n}}\hat{\mathbf{n}}$.

In addition, kinematic boundary condition $\hat{\mathbf{n}} \cdot \mathbf{u} = 0$ is enforced at the free surface in the mesh, such as there is no mass flux across the interface, and the static contact line location is specified in order to solve the mesh equation (Pasquali and Scriven, 2002).

2.2 Boussinesq-Scriven model

A constitutive equation for the interfacial stress tensor at the free-surface boundary condition is required. Because most slot coating research uses simple interfaces, several stress-related interfacial effects are often overlooked. The Boussinesq-Scriven model, an early constitutive model proposed by Boussinesq (1913) and later formalized by Scriven (1960), is used in this work and can be interpreted as an equivalent of the Newtonian constitutive equation for bulk fluids at the interface. The interfacial stress tensor, in this model, is given by:

$$\sigma_\mathbf{s} = \zeta\mathbf{I} + \kappa_\mathbf{s}(\nabla_s \cdot \mathbf{u_s})\mathbf{I_s} + 2\mu_s\mathbf{D_s^{dev}} \tag{4}$$

where ζ is the interfacial tension and κ_s and μ_s are the coefficients of interfacial dilatational viscosity and interfacial shear viscosity, respectively, in which dimensions differ from fluid viscosity.

In equation 4, the term $\mathbf{D_s^{dev}}$ refers to the deviatoric part of the rate-of-strain interfacial tensor, that can be writen as:

$$\mathbf{D_s^{dev}} = \mathbf{D_s} - \frac{1}{2}(\nabla_s \cdot \mathbf{u_s})\mathbf{I}_s \tag{5}$$

where the surface velocity divergence $\nabla_s \cdot \mathbf{u_s} = \mathbf{I_s} : \mathbf{D_s}$ and the surface rate-of-strain tensor is $\mathbf{D_s} = \frac{1}{2}(\nabla_s\mathbf{u_s} \cdot \mathbf{I_s} + \mathbf{I_s} \cdot \nabla_s\mathbf{u^T})$.

The flow is modeled as a two-dimensional planar flow, simplifying the constitutive model and its associated interfacial traction. In this case, the fluid-fluid interface is one-dimensional, the basis vectors can be set at any point located at the interface and the arclength coordinate along the interface (s) is introduced. It results in the following mathematical simplifications (Mendes Junior *et al.*, 2021; Silva *et al.*, 2023):

1. The interfacial velocity is written as $\mathbf{u} = u_t\hat{\mathbf{t}}$, where $u_t = \mathbf{u} \cdot \hat{\mathbf{t}}$ is the velocity component tangent to the interface;
2. The projection tensor takes the form $\mathbf{I_s} = \hat{\mathbf{t}}\hat{\mathbf{t}} + \hat{\mathbf{k}}\hat{\mathbf{k}}$, where $\hat{\mathbf{t}}$ and $\hat{\mathbf{k}}$ are respectively the local unit tangent and spanwise direction vectors.
3. The surface gradient operator is $\nabla_s(...) = \hat{t}\frac{d}{ds}(...)$, where s is the arclength coordinate along the interface, previously introduced.
4. As a consequence of the previous item, the surface velocity divergence becomes $\nabla_s \cdot \mathbf{u} = \frac{du_t}{ds}$ and the rate-of-strain and its deviatoric part becomes $\mathbf{D_s} = \frac{du_t}{ds}(\hat{\mathbf{t}}\hat{\mathbf{t}})$ and $\mathbf{D_s^{dev}} = \frac{1}{2}\frac{du_t}{ds}(\hat{\mathbf{t}}\hat{\mathbf{t}} - \hat{\mathbf{k}}\hat{\mathbf{k}})$ respectively.

Using the simplifications above, the interfacial stress tensor and its surface divergent in the Boussinesq-Scriven model is given by

$$\sigma_\mathbf{s} = [\zeta + (\kappa_s + \mu_s)\frac{du_t}{ds}]\hat{\mathbf{t}}\hat{\mathbf{t}} + [\zeta + (\kappa_s - \mu_s)\frac{du_t}{ds}]\hat{\mathbf{k}}\hat{\mathbf{k}} \tag{6}$$

$$\nabla_s \cdot \sigma_\mathbf{s} = (\zeta + \eta_s\frac{du_t}{ds})\frac{d\hat{\mathbf{t}}}{ds} + (\frac{d\zeta}{ds} + \frac{d\eta_s}{ds}\frac{du_t}{ds} + \eta_s\frac{d^2u_t}{ds^2})\hat{\mathbf{t}} \tag{7}$$

In equation 7, η_s is the sum of the dilatational and shear interfacial viscosities, turning out to be the only material property on two-dimensional planar flows. It is assumed that both the interfacial stress tensor and the total interfacial viscosity are constants. As a result, the interfacial force balance is reduced to:

$$\mathbf{n} \cdot \sigma = -p_0 \hat{\mathbf{n}} + \eta_s \frac{d^2 u_t}{ds^2} \hat{\mathbf{t}} + (\zeta + \eta_s \frac{du_t}{ds}) \frac{d\hat{\mathbf{t}}}{ds} \tag{8}$$

We notice here that the presence of a viscous interface has contributions in the normal (in addition to surface tension) and tangential directions.

2.3 Dimensionless numbers

A dimensionless analysis of the problem indicates the convenience of the introduction of four dimensionless numbers to describe the coating flow:

1. The Reynolds number: $Re = \rho V H/\mu$
2. The Capillary number: $Ca = \mu V/\sigma$
3. The Boussinesq number: $Bq = \eta_s/\mu H$
4. The dimensionless flow rate: $Q = h/H$

Here, ρ is the density of the coating liquid, and μ its bulk viscosity. V and H are the characteristic scales of velocity and length, respectively, whereas h is the film thickness. As stated before, we are interested in free surface flows that occur on a small scale and often exhibit minimal inertial effects; hence, the flow is inertialess and Re is assumed to be zero.

2.4 Numerical Formulation

To solve the free surface, the elliptic mesh generation method (De Santos, 1991) was used, which involved coupling the equations of motion and boundary conditions. This method is extensively employed in solutions of Newtonian (Carvalho and Kheshgi, 2000; Soares and Thompson, 2009; Freitas *et al.*, 2011b; Mendes Junior *et al.*, 2021; Silva *et al.*, 2023) and Non-Newtonian (Pasquali and Scriven, 2002; Romero *et al.*, 2004, 2006; Bajaj *et al.*, 2008; Freitas *et al.*, 2011a; Thompson and Soares, 2012; Freitas *et al.*, 2013; Siqueira *et al.*, 2017; Siqueira and Carvalho, 2017) liquids. The resulting system consisted of nonlinear partial differential equations for velocity, pressure, and mesh position. To discretize this system, a mixed finite element formulation was employed. Each unknown field variable is expressed as a linear combination of a finite number of basis functions: linear discontinuous for pressure and Lagrangian biquadratic for velocity and mesh position. Galerkin's weighting functions are employed in the residual formulation of all equations, namely mass conservation, momentum balance, and mesh generation. The integrals are solved element by element using Gaussian quadrature, and the fully-coupled solution is computed using Newton's method and a numerical Jacobian matrix. At each iteration, the linear system is solved with a LU frontal solver (Duff *et al.*, 1989) and the tolerance on the 2-norm of the global residual vector. The last Newton's update is set to 10^{-6} and solutions at different values of parameters are achieved with a first-order pseudo-arc-length continuation scheme (Bolstad and Keller, 1986). Since Newton's method requires an adequate initial solution, the first solution used was a fixed boundary flow field with a slippery wall in place of the free surface (Romero *et al.*, 2004).

The flow domain was discretized into 1782 quadrilateral elements, consisting of 7327 nodes and 34,654 degrees of freedom. Readers can find a detailed description of the mesh and the mesh convergence test in Silva *et al.* (2023).

3. RESULTS

As previously stated, the flow is inertialess, and the results reported in this section are dimensionless, with capillary and Boussinesq numbers being the key parameters varied in the results below. The effects of a viscous liquid-gas interface at the free surface of the downstream meniscus in a slot coating flow are investigated using the Boussinesq-Scriven model. In this study, we showcase a series of results that illustrates how viscous interfaces influence the dynamics of slot coating flow for Newtonian bulk liquids. Downstream of the die lip, the flow in the film assumes rigid-body motion while upstream of the die lip the flow can be summarized as a combination of pressure-driven (Poiseuille) and boundary-driven (Couette) flows. As the film thickness decreases, the contribution of the adverse pressure gradient-driven flow increases, increasing the curvature of the downstream meniscus, intrinsically depending on the Ca and Q. For Newtonian fluids, it is observed that at $Q = 1/2$, there is no contribution due to an adverse pressure, and the flow under the downstream slot die is a pure drag flow. In contrast, at $Q \leq 1/3$ for example, there is a large contribution from the adverse pressure gradient, and backflow occurs close to the meniscus. This arises from an integral mass balance applied around the slot coater and it

is noteworthy that this kinematic constraint remains valid for Newtonian bulk liquids regardless of liquid properties and interfacial rheology.

Figures 2 and 3 depict the velocity field and flow streamlines towards the end of the downstream slot die for various Ca and Bq values, with the dimensionless flow set at $Q = 0.3$ and $Q = 0.5$. In the first column, we can observe the recirculation zone at the upper section of the flow near the meniscus since the flow rate is less than $1/3$ while in the second column, where the flow rate is equal to $1/2$, there is no backflow. As the capillary number rises, the viscous forces in the bulk liquid outweigh the surface tension forces, and the meniscus' curvature increase as the surface tension fall - this effect is less pronounced for high Bq. On the other hand, when we fix Ca and increase Bq, we observe that the curvature of the meniscus reduces and the flow slows down and is developed at a later point, as illustrated in figure 3.

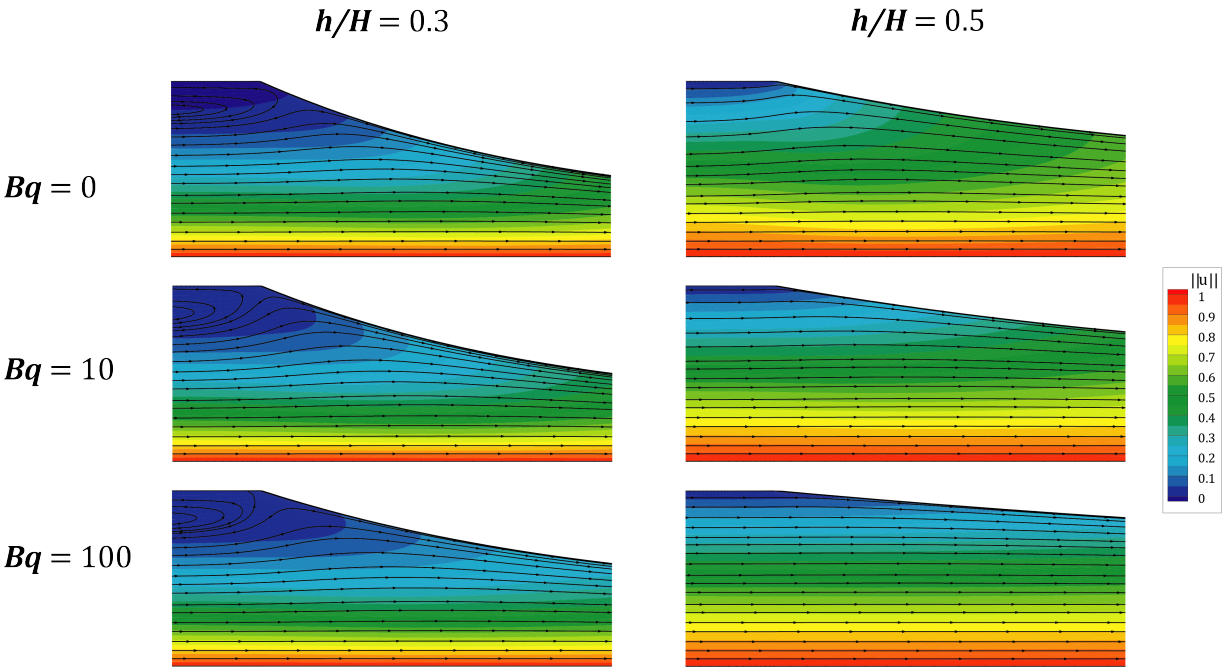

Figure 2. Magnitude of velocity field and flow streamlines at the beginning of the film formation region ($-0.5 \leq x \leq 2$; $0 \leq y \leq 1$) for $Q = 0.3$ and $Q = 0.5$ at $Ca = 0.01$

Figures 4, 5 and 6 depicts the position y, the streamwise component of the velocity u, and the surface divergence of the interfacial velocity along the interface du_t/ds of the downstream meniscus for a set of Ca and Bq for the adimensional flow rate of $Q = 0.3$ and $Q = 0.5$. The plot begins at the static contact line, and the relationship between the meniscus' curvature and the capillary and Boussinesq numbers, as previously discussed, is readily seen in figures 2 and 3. The liquid acceleration along the free surface is prevented by the interfacial viscosity and in order to maintain the mass flow rate imposed at the inlet, the free surface must increase since the liquid flows more slowly when the liquid-gas interface is viscous. This is consistent with previous research on extrudate swell flows (Mendes Junior *et al.*, 2021) and slot coating (Silva *et al.*, 2023). It should be noted that the film thickness in the fully developed region is known a priori as the slot coating is a pre-metered method.

Figure 5 shows the u velocity at the free surface for $Q = 0.3$ and $Q = 0.5$ and we can notice some backflow, i.e., velocities where $u < 0$ exactly at the meniscus's commencement but only when $Bq = 0$ and $Q = 0.3$. Because of the no-slip condition, the interfacial velocity starts at zero and grows along the substrate until it reaches its maximum value as the flow develops and assumes rigid body motion, where the velocity of the meniscus equals the substrate velocity. As expected, as Ca increases, the meniscus bends more and becomes more flexible as its surface tension lowers, causing the film flow to be fully developed at earlier positions. This effect is less noticeable on high Bq numbers, as the viscous interface slows down the flow and requires longer substrate length to develop the film flow.

At last, figure 6 illustrates a significant jump of values of the interfacial velocity's derivative along the arc length at the beginning of the free surface when the interface is simple ($Bq = 0$) for both dimensionless flow rates. As the interface becomes more viscous, the acceleration of the fluid as it leaves the downstream die lip becomes smaller, indicating greater resistance to surface deformations. In this sense, the surface stretches and it takes longer lengths for the surface velocity gradient to become null, leading to the film flow developing at longer lengths.

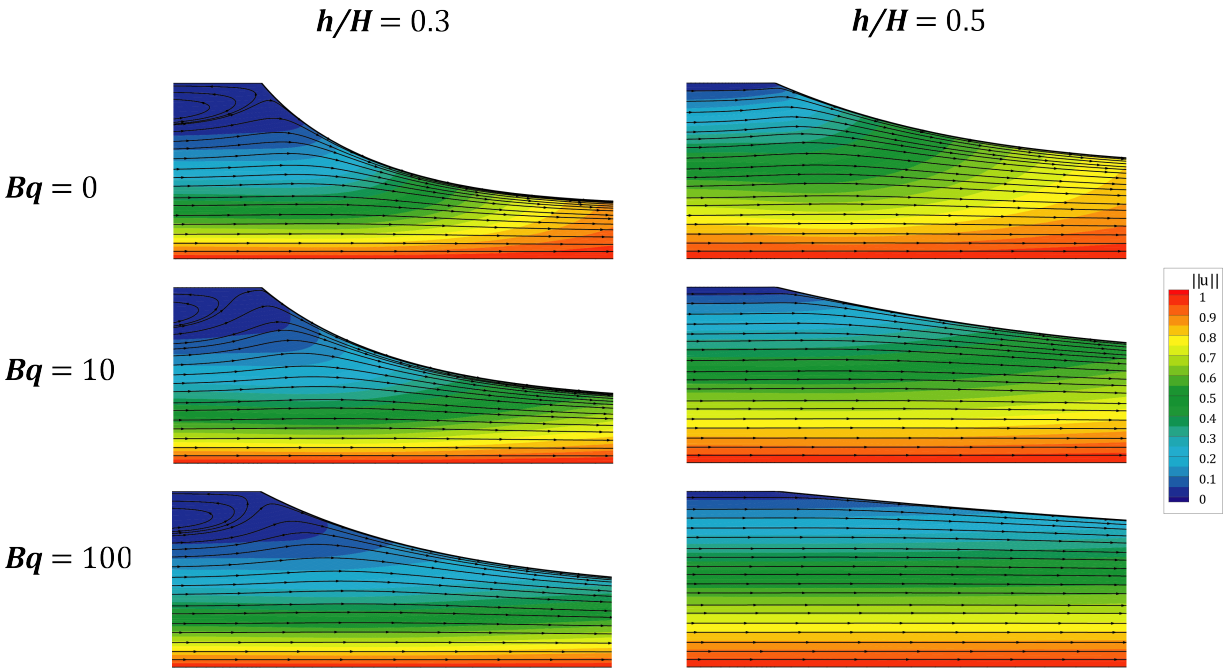

Figure 3. Magnitude of velocity field and flow streamlines at the beginning of the film formation region ($-0.5 \leq x \leq 2$; $0 \leq y \leq 1$) for $Q = 0.3$ and $Q = 0.5$ at $Ca = 0.1$.

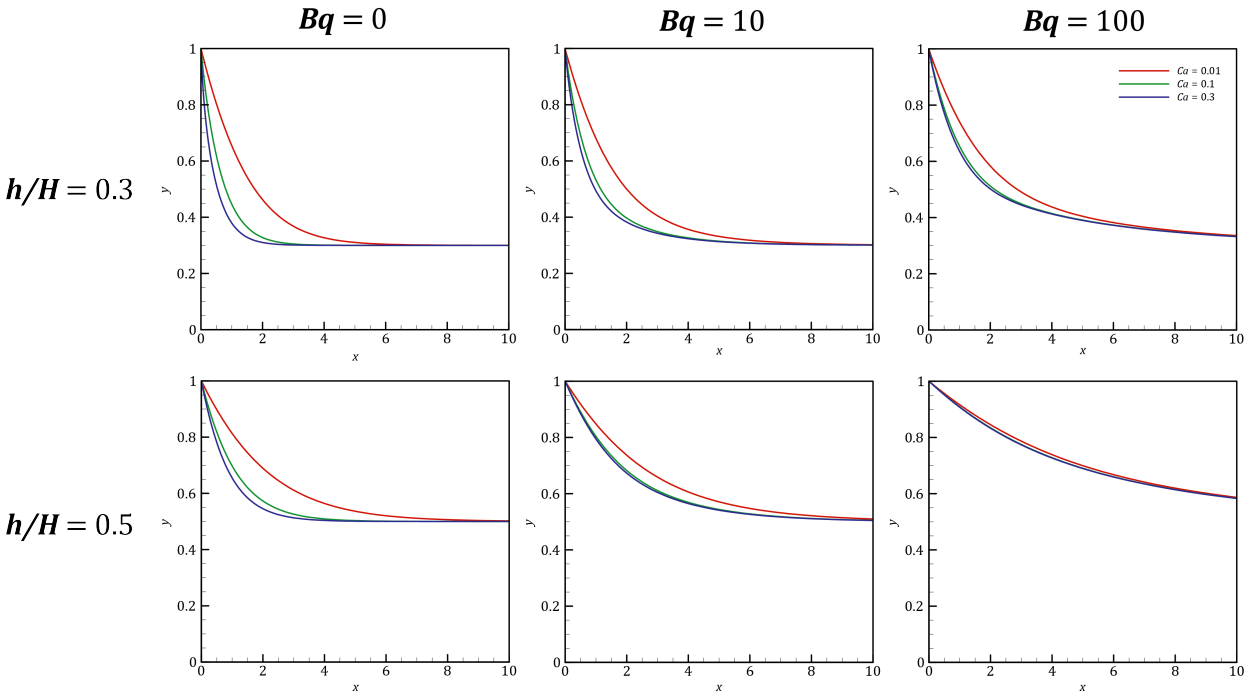

Figure 4. Shape of the free surface for $Q = 0.3$ and $Q = 0.5$ for different Ca and Bq numbers.

4. CONCLUSIONS

Slot coating is a pre-metered coating process highly used in various manufacturing processes. Although numerous research in literature have addressed the role played by the rheology of the bulk coating liquid, it is still not entirely clear how rheologically complex interfaces influence free surface flows such as slot coating. In this study, we extend the existing literature by conducting a computational investigation of free surface flows with viscous interfaces in the film formation region, specifically focusing on the downstream section of a slot coater.

The current study conducted a numerical investigation of the slot coating flow and its operating conditions while mod-

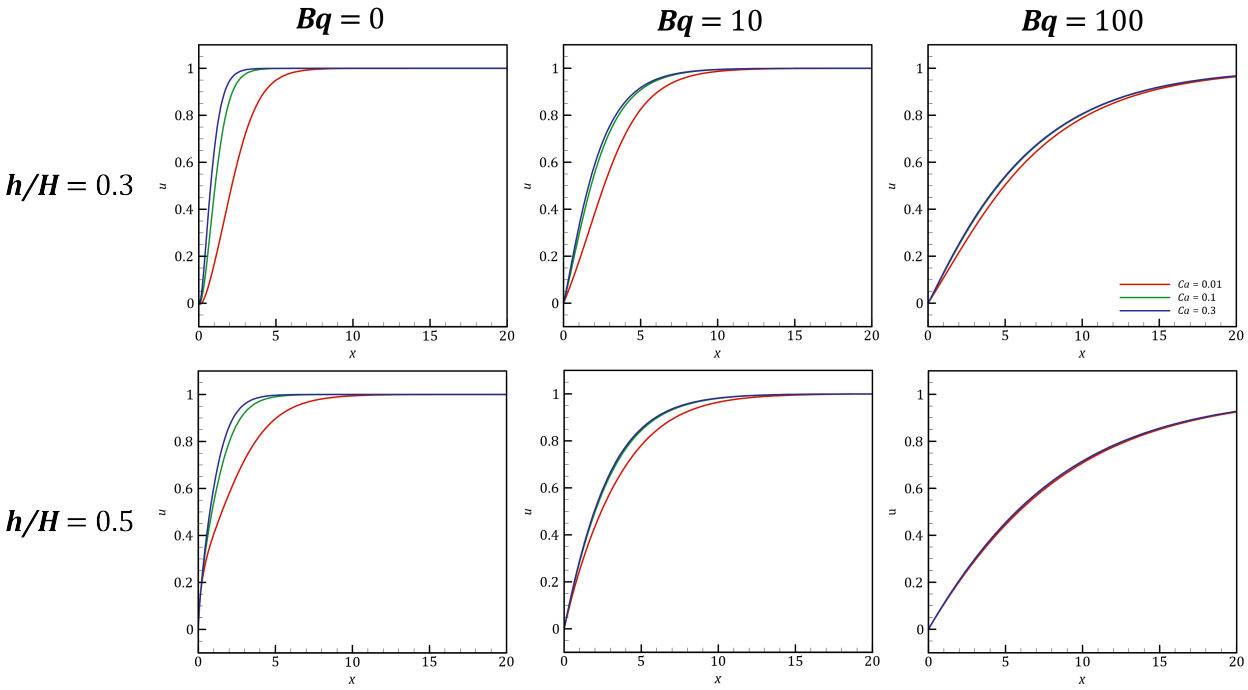

Figure 5. Streamwise velocity along the free surface for $Q = 0.3$ and $Q = 0.5$ for different Ca and Bq numbers.

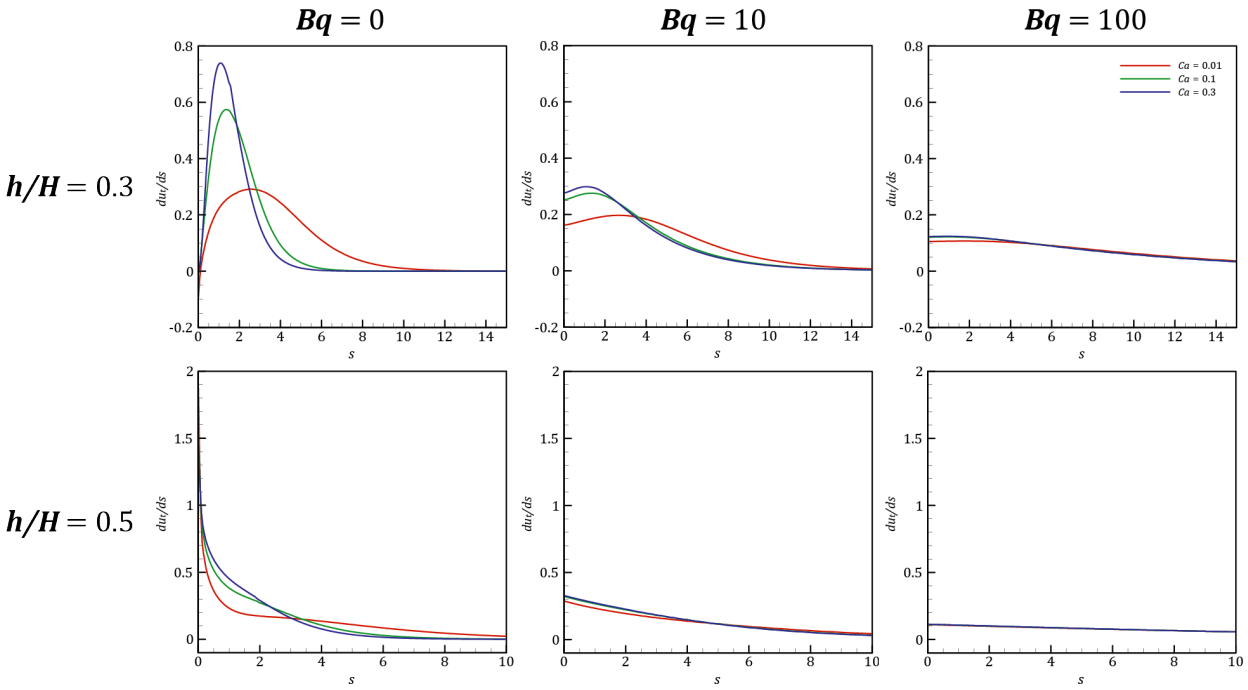

Figure 6. Interfacial velocity divergence along the free surface for $Q = 0.3$ and $Q = 0.5$ for different Ca and Bq numbers.

eling its free surface as a liquid-gas interface defined by the Boussinesq-Scriven model with an incompressible Newtonian bulk liquid. To capture the free surfaces, Galerkin's finite element method was used in conjunction with the elliptic mesh generation method to solve the resulting set of equations governing the steady, two-dimensional slot coating flow coupled with an appropriate viscous, Newtonian-like interface boundary condition.

The results showed that, for both dimensionless flow rates, the viscous interface leads to a less curved meniscus and more required substrate length to develop the film flow as the flow in both the bulk flow and the interface is hindered by the interfacial viscosity. The parametric study revealed that this behavior was consistent for different capillary numbers and for higher capillary numbers, the free surface bends more but it leads to less required substrate length to develop the film flow. This behavior also influences other variables studied, namely the streamwise velocity and the interfacial velocity

divergence as both of these parameters show less influence from the surface tension as Boussinesq numbers increase.

5. ACKNOWLEDGEMENTS

This study was supported by the Coordenação de Aperfeiçoamento de Pessoal de Nıvel Superior (CAPES) from the Brazilian Ministry of Education (MEC) under Grant No. PROEX 803/2018 and the Industrial Partnership for Research in Interfacial Materials and Engineering (IPRIME) at the University of Minnesota.

6. REFERENCES

Bajaj, M., Prakash, J.R. and Pasquali, M., 2008. "A computational study of the effect of viscoelasticity on slot coating flow of dilute polymer solutions". *Journal of Non-Newtonian Fluid Mechanics*, Vol. 149, No. 1-3, pp. 104–123.

Beguin, A.E., 1954. "Method of coating strip material". *U.S. Patent No. 2,681,294*.

Benkreira, H. and Ikin, J.B., 2016. "Slot coating minimum film thickness in air and in rarefied helium". *Chemical Engineering Science*, Vol. 150, pp. 66–73.

Bolstad, J.H. and Keller, H.B., 1986. "A multigrid continuation method for elliptic problems with folds". *SIAM J Sci Stat Comput.*, Vol. 7, pp. 1081–1104.

Boussinesq, J., 1913. "Existence of a superficial viscosity in the thin transition layer separating one liquid from another contiguous fluid". *C R Acad Sci.*, Vol. 156, pp. 983–989.

Campana, D.M., Silva, L.D.V. and Carvalho, M.S., 2017. "Slot coating flows of non-colloidal particle suspensions". *AIChE J.*, Vol. 63 (3), p. 1122–1131.

Carvalho, M.S. and Kheshgi, H.S., 2000. "Low-flow limit in slot coating: theory and experiments". *AIChE Journal*, Vol. 46, No. 10, pp. 1907–1917.

Chang, Y.R., Chang, H.M., Lin, C.F., Liu, T.J. and Wu, P.Y., 2007. "Three minimum wet thickness regions of slot die coating". *Journal of Colloid and Interface Science*, Vol. 308, No. 1, pp. 222–230.

Conrado, H., Dias, E.O. and Miranda, J.A., 2023. "Impact of interfacial rheology on finger tip splitting". *Physical Review E*, Vol. 107, No. 1, p. 015103.

Coutinho, I.M., Dias, E.O. and Miranda, J.A., 2023. "Effect of interfacial rheology on fingering patterns in rotating Hele-Shaw cells". *Physical Review E*, Vol. 107, No. 2, p. 025105.

De Santos, J.M., 1991. "Two-phase cocurrent downflow through constricted passages [phd dissertation]". *Minneapolis, Minnesota: University of Minnesota.*

Duff, I.S., Erisman, A.M. and Reid, J.K., 1989. "Direct methods for sparse matrices". *Oxford University Press*, Vol. 1st ed.

Freitas, J.F., Soares, E.J. and Thompson, R.L., 2011a. "Immiscible newtonian displacement by a viscoplastic material in a capillary plane channel". *Rheol Acta.*, Vol. 50, pp. 403–422.

Freitas, J.F., Soares, E.J. and Thompson, R.L., 2011b. "Residual mass and flow regimes for the immiscible liquid–liquid displacement in a plane channel". *International Journal of Multiphase Flow.*, Vol. 37, pp. 640–646.

Freitas, J.F., Soares, E.J. and Thompson, R.L., 2013. "Viscoplastic–viscoplastic displacement in a plane channel with interfacial tension effects". *Chemical Engineering Science.*, Vol. 91, pp. 54–64.

Fuller, G.G. and Vermant, J., 2012. "Complex fluid–fluid interfaces: rheology and structure". *Annu Rev Chem Biomol Eng.*, Vol. 3, pp. 519–543.

Jaensson, N. and Vermant, J., 2018. "Tensiometry and rheology of complex interfaces". *Curr Opin Colloid Interface Sci.*, Vol. 37, pp. 136–150.

Jaensson, N.O., Anderson, P.D. and Vermant, J., 2021. "Computational interfacial rheology". *J Non-Newtonian Fluid Mech.*, Vol. 290, p. 104507.

Khandavalli, S. and Rothstein, J.P., 2016. "The effect of shear-thickening on the stability of slot-die coating". *AIChE Journal*, Vol. 62, No. 12, pp. 4536–4547.

Kwak, H. and Nam, J., 2020. "Simple criterion for vortex formation in the channel flow of power-law fluids". *Journal of Non-Newtonian Fluid Mechanics*, Vol. 284, p. 104372.

Kwak, H. and Nam, J., 2022. "Effect of slot-die configurations on coating gap dependence of maximum and minimum wet thicknesses". *AIChE Journal*, Vol. 68, No. 9, p. e17745.

Lee, K.Y. and Liu, T.J., 1992. "Minimum web thickness in extrusion slot coating". *Chem. Eng. Sci.*, Vol. 47, p. 1703–1713.

Lee, S. and Nam, J., 2015. "Analysis of slot coating flow under tilted die". *AIChE Journal*, Vol. 61, No. 5, pp. 1745–1758.

Lee, S. and Nam, J., 2017. "Transient response of slot coating flows of shear-thinning fluids to periodic disturbances". *Journal of Coatings Technology and Research*, Vol. 14, No. 5, pp. 981–990.

Lee, S.H., Koh, H.J., Ryu, B.K., Kim, S.J., Jung, H.W. and Hyun, J.C., 2011. "Operability coating windows and frequency response in slot coating flows from a viscocapillary model". *Chemical Engineering Science*, Vol. 66, No. 21, pp. 4953–4959.

Li, J. and Manikantan, H., 2021. "Influence of interfacial rheology on viscous fingering". *Physical Review Fluids*, Vol. 6,

No. 7, p. 074001.

Martínez-Calvo, A. and Sevilla, A., 2018. "Temporal stability of free liquid threads with surface viscoelasticity". *Journal of Fluid Mechanics*, Vol. 846, pp. 877–901.

Martínez-Calvo, A. and Sevilla, A., 2020. "Universal thinning of liquid filaments under dominant surface forces". *Physical Review Letters*, Vol. 125, No. 11, p. 114502.

Mendes Junior, P.R.C., Siqueira, I.R., Thompson, R.L. and Carvalho, M.S., 2021. "Computational study of planar extrudate swell flows with a viscous liquid–gas interface". *AIChE J.*, Vol. e17503.

Narsimhan, V., 2018. "The effect of surface viscosity on the translational speed of droplets". *Physics of Fluids*, Vol. 30, No. 8, p. 081703.

Narsimhan, V., 2019. "Shape and rheology of droplets with viscous surface moduli". *Journal of Fluid Mechanics*, Vol. 862, pp. 385–420.

Papanastasiou, T.C., Malamataris, N. and Ellwood, K., 1992. "A new outflow boundary condition". *Int J Numer Methods Fluids.*, Vol. 14, pp. 587–608.

Pasquali, M. and Scriven, L.E., 2002. "Free surface flows of polymer solutions with models based on the conformation tensor". *Journal of Non-Newtonian Fluid Mechanics*, Vol. 108, No. 1-3, pp. 363–409.

Rebouças, R.B., Siqueira, I.R. and S., C.M., 2018. "Slot coating flow of particle suspensions: particle migration in shear sensitive liquids." *J Non-Newtonian Fluid Mech.*, Vol. 258, pp. 22–31.

Romero, O.J., Scriven, L.E. and Carvalho, M.S., 2006. "Slot coating of mildly viscoelastic liquids". *Journal of Non-Newtonian Fluid Mechanics*, Vol. 138, No. 2-3, pp. 63–75.

Romero, O.J., Suszynski, W.J., Scriven, L.E. and Carvalho, M.S., 2004. "Low-flow limit in slot coating of dilute solutions of high molecular weight polymer". *Journal of Non-Newtonian Fluid Mechanics*, Vol. 118, No. 2-3, pp. 137–156.

Rong, Y., Ming, Y., Ji, W., Li, D., Mei, A., Hu, Y. and Han, H., 2018. "Toward industrial-scale production of perovskite solar cells: screen printing, slot-die coating, and emerging techniques". *The Journal of Physical Chemistry Letters*, Vol. 9, No. 10, pp. 2707–2713.

Sartor, L., 1990. "Slot coating: fluid mechanics and die design [phd dissertation]". *Minneapolis, Minnesota: University of Minnesota*.

Schmitt, M., Baunach, M., Wengeler, L., Peters, K., Junges, P., Scharfer, P. and Schabel, W., 2013. "Slot-die processing of lithium-ion battery electrodes–coating window characterization". *Chemical Engineering and Processing: Process Intensification*, Vol. 68, pp. 32–37.

Schmitt, M., Diehm, R., Scharfer, P. and Schabel, W., 2015. "An experimental and analytical study on intermittent slot die coating of viscoelastic battery slurries". *Journal of Coatings Technology and Research*, Vol. 12, No. 5, pp. 927–938.

Schmitt, M., Scharfer, P. and Schabel, W., 2014. "Slot die coating of lithium-ion battery electrodes: investigations on edge effect issues for stripe and pattern coatings". *Journal of Coatings Technology and Research*, Vol. 11, No. 1, pp. 57–63.

Scriven, L.E., 1960. "Dynamics of a fluid interface equation of motion for newtonian surface fluids". *Chem Eng Sci.*, Vol. 12, pp. 98–108.

Silva, F.O., Siqueira, I.R., Carvalho, M.S. and Thompson, R.L., 2023. "Slot coating flows with a boussinesq–scriven viscous interface". *Phys. Fluids*, Vol. 35, p. 042106.

Singh, N. and Narsimhan, V., 2020. "Deformation and burst of a liquid droplet with viscous surface moduli in a linear flow field". *Physical Review Fluids*, Vol. 5, No. 6, p. 063601.

Siqueira, I.R. and Carvalho, M.S., 2017. "Particle migration in planar die-swell flows". *J Fluid Mech.*, Vol. 825, pp. 49–68.

Siqueira, I.R. and Carvalho, M.S., 2019. "A computational study of the effect of particle migration on the low-flow limit in slot coating of particle suspensions". *J Coatings Technol Res.*, Vol. 16, pp. 1619–1628.

Siqueira, I.R., Rebouças, R.B. and Carvalho, M.S., 2017. "Particle migration and alignment in slot coating flows of elongated particle suspensions". *AIChE J.*, Vol. 63, pp. 3187–3198.

Soares, E.J. and Thompson, R.L., 2009. "Flow regimes for the immiscible liquid–liquid displacement in capillary tubes with complete wetting of the displaced liquid". *J. Fluid Mech.*, Vol. 641, pp. 63–84.

Thompson, R.L. and Soares, E.J., 2012. "Motion of a power-law long drop in a capillary tube filled by a newtonian fluid". *Chemical Engineering Science.*, Vol. 72, pp. 126–141.

Verma, A., Martineau, D., Hack, E., Makha, M., Turner, E., Nüesch, F. and Heier, J., 2020. "Towards industrialization of perovskite solar cells using slot die coating". *Journal of Materials Chemistry C*, Vol. 8, No. 18, pp. 6124–6135.

Wee, H., Wagoner, B.W., Kamat, P.M. and Basaran, O.A., 2020. "Effects of surface viscosity on breakup of viscous threads". *Physical Review Letters*, Vol. 124, No. 20, p. 204501.

Whitaker, J.B., Kim, D.H., Larson, B.W., Zhang, F., Berry, J.J., Van Hest, M.F.A.M. and Zhu, K., 2018. "Scalable slot-die coating of high performance perovskite solar cells". *Sustainable Energy & Fuels*, Vol. 2, No. 11, pp. 2442–2449.

Yoon, J., Kim, D., Lee, S.H., Kang, D. and Nam, J., 2022. "Simplified model for operability window of slot coating without vacuum". *Chemical Engineering Science*, Vol. 259, p. 117766.

7. RESPONSIBILITY NOTICE

The authors are solely responsible for the printed material included in this paper.